40-Gbaud 16-QAM transmitter using tandem IQ modulators with binary driving electronic signals

Guo-Wei Lu,[1,*] Mats Sköld,[2] Pontus Johannisson,[1] Jian Zhao,[3] Martin Sjödin,[1] Henrik Sunnerud,[2] Mathias Westlund,[2] Andrew Ellis,[3] and Peter A. Andrekson[1,2]

[1]*Photonics Laboratory, Department of Microtechnology and Nanoscience (MC2), Chalmers University of Technology, SE- 412 96 Göteborg, Sweden*
[2]*EXFO Sweden AB, Arvid Hedvalls Backe 4, SE-411 33 Göteborg, Sweden*
[3]*Photonic Systems Group, Tyndall National Institute and Department of Physics, University College Cork, Lee Maltings, Prospect Row, Cork, Ireland*
*guowei@chalmers.se

Abstract: We propose a novel 16-quadrature amplitude modulation (QAM) transmitter based on two cascaded IQ modulators driven by four separate binary electrical signals. The proposed 16-QAM transmitter features scalable configuration and stable performance with simple bias-control. Generation of 16-QAM signals at 40 Gbaud is experimentally demonstrated for the first time and visualized with a high speed constellation analyzer. The proposed modulator is also compared to two other schemes. We investigate the modulator bandwidth requirements and tolerance to accumulated chromatic dispersion through numerical simulations, and the minimum theoretical insertion attenuation is calculated analytically.

©2010 Optical Society of America

OCIS codes: (060.4510) Optical communications; (060.5060) Phase modulation.

References and links

1. A. Sano, H. Masuda, T. Kobayashi, M. Fujiwara, K. Horikoshi, E. Yoshida, Y. Miyamoto, M. Matsui, M. Mizoguchi, H. Yamazaki, Y. Sakamaki, and H. Ishii, "69.1-Tb/s (432 x 171-Gb/s) C- and Extended L-Band Transmission over 240 Km Using PDM-16-QAM Modulation and Digital Coherent Detection," in *Optical Fiber Communication Conference*, OSA Technical Digest (CD) (Optical Society of America, 2010), paper PDPB7. *http://www.opticsinfobase.org/abstract.cfm?URI=OFC-2010-PDPB7*
2. Y. K. Huang, E. Ip, M.-F. Huang, B. Zhu, P. N. Ji, Y. Shao, D. W. Peckham, R. Lingle, Y. Aono, T. Tajima, and T. Wang, "10x456-Gb/s DP-16QAM transmission over 8x100 km of ULAF using coherent detection with a 30-GHz Analog-to-Digital Converter," in Proc. OECC, paper PD3, 2010.
3. M. Nakazawa, S. Okamoto, T. Omiya, K. Kasai, and M. Yoshida, "256 QAM (64 Gbit/s) Coherent Optical Transmission over 160 km with an Optical Bandwidth of 5.4 GHz," in *Optical Fiber Communication Conference*, OSA Technical Digest (CD) (Optical Society of America, 2010), paper OMJ5. *http://www.opticsinfobase.org/abstract.cfm?URI=OFC-2010-OMJ5*
4. K.-P. Ho, and H.-W. Cuei, "Generation of Arbitrary Quadrature Signals using One Dual-Drive Modulator," J. Lightwave Technol. **23**(2), 764–770 (2005), http://www.opticsinfobase.org/JLT/abstract.cfm?URI=JLT-23-2-764.
5. P. J. Winzer, A. H. Gnauck, C. R. Doerr, M. Magarini, and L. L. Buhl, "Spectrally Efficient Long-Haul Optical Networking Using 112-Gb/s Polarization-Multiplexed 16-QAM," J. Lightwave Technol. **28**(4), 547–556 (2010), http://www.opticsinfobase.org/JLT/abstract.cfm?URI=JLT-28-4-547.
6. Y. Mori, C. Zhang, K. Igarashi, K. Katoh, and K. Kikuchi, "Unrepeated 200-km transmission of 40-Gbit/s 16-QAM signals using digital coherent receiver," Opt. Express **17**(3), 1435–1441 (2009), http://www.opticsinfobase.org/abstract.cfm?URI=oe-17-3-1435.
7. T. Sakamoto, A. Chiba, and T. Kawanishi, "50-Gb/s 16 QAM by a quad-parallel Mach-Zehnder modulator," in Proc. ECOC 2007, paper PD2.8, 2007.
8. H. Yamazaki, T. Yamada, T. Goh, Y. Sakamaki, and A. Kaneko, 64QAM modulator with a hybrid configuration of silica PLCs and LiNbO$_3$ phase modulators for 100-Gb/s applications," in Proc. ECOC 2009, paper 2.2.1, 2009.
9. X. Zhou, and J. Yu, "200-Gb/s PDM-16QAM generation using a new synthesizing method," in Proc. ECOC 2009, paper 10.3.5, 2009.
10. X. Zhou, and J. Yu, "Multi-Level, Multi-Dimensional Coding for High-Speed and High-Spectral-Efficiency Optical Transmission," J. Lightwave Technol. **27**(16), 3641–3653 (2009), http://www.opticsinfobase.org/abstract.cfm?URI=JLT-27-16-3641.
11. M. Seimetz, "Transmitter design," in *High-order modulation for optical fiber transmission*, (Springer, 2009), pp. 28.

12. M. Seimetz, "Performance of Coherent Optical Square-16-QAM-Systems Based on IQ-Transmitters and Homodyne Receivers with Digital Phase Estimation," in *Optical Fiber Communication Conference and Exposition and The National Fiber Optic Engineers Conference*, Technical Digest (CD) (Optical Society of America, 2006), paper NWA4. *http://www.opticsinfobase.org/abstract.cfm?URI=NFOEC-2006-NWA4*

1. Introduction

With the increasing data rate demands on optical transport networks, advanced optical multi-level modulation formats, such as orthogonal frequency-division multiplexing (OFDM) and quadrature amplitude modulation (QAM), are promising candidates to provide high spectral efficiency in optical communication systems. Both single-carrier and multi-tone multilevel modulation formats have attracted much research attention for enabling the ultra-fast and ultra-dense optical transmission systems. Polarization-multiplexed 16-QAM at 21.4 Gbaud [1], dual-polarization optical-time-division-multiplexing 16-QAM at 57 Gbaud [2], and 256-QAM at 4 Gbaud [3] have been experimentally demonstrate to achieve an aggregate bit-rate of up to 69.1 Tbit/s and a spectral efficiency of 11.8 bit/s/Hz. So far, the reported QAM transmitter schemes could be categorized into three groups: i) single Mach-Zehnder modulator (MZM) or in-phase/quadrature (IQ) modulator driven by multi-level electrical signals [2–6]; ii) highly integrated modulators with binary electrical driving signals, which integrate at least four sub-MZMs in parallel in one device [1,7,8]; iii) cascade of a phase modulator (PM) with an IQ modulator and MZM modulators in series [9–11]. However, these techniques suffer from the following problems to generate a high-quality QAM signal: i) much more stringent bandwidth requirements of both the modulator and the electrical drivers when handling multi-level electrical driving signals; ii) high complexity with high-order optical integration; iii) reduced tolerance against dispersion and modulation bandwidth limitations caused by additional chirp due to the use of a PM.

Instead of using higher-order optical integration or multi-level electrical driving signals, utilization of commercially available IQ modulators and binary electrical driving signals would facilitate the generation of advanced optical modulation formats. In this paper, we propose and experimentally demonstrate a novel 16-QAM transmitter using two tandem IQ modulators driven by four binary electrical signals. Numerical simulations are used to investigate the modulator bandwidth requirements and the tolerance against accumulated chromatic dispersion, in comparison to selected previous schemes. A comparison of the theoretical insertion attenuation is also presented. For the first time, we successfully generate and analyze up to 40-Gbaud 16-QAM signals. We characterize the signal with an ultra high-speed optical modulation analyzer that ensures the recovery of the true constellations and transitions. No digital signal processing (DSP) for inter-symbol interference (ISI) mitigation is used. It features stable performance and potentially low cost.

2. Operation principle

Figure 1 depicts the operation principle of the proposed 16-QAM transmitter, which consists of two IQ modulators in series. Four independent binary electrical signals are employed to drive the two IQ modulators. In one of the IQ modulators, both sub-MZMs are under-driven with peak-to-peak swings of around 0.8 V_π and biased at the positive inflection with a 0.6 V_π offset from the transmission null, generating an offset 4-QAM in one quadrature of the complex plane. The two sub-MZMs in the other IQ modulator are fully-driven by $2V_\pi$ and biased at the transmission null to obtain quadrature phase modulation states, i.e. QPSK. After cascading these two IQ modulators in series, the modulation introduced by the fully-driven second IQ modulator will map the offset 4-QAM constellation to the four different quadratures, thereby obtaining a complete 16-QAM constellation. Note that, in the proposed scheme, the order of the two cascaded IQ modulators will not affect transmitter performance.
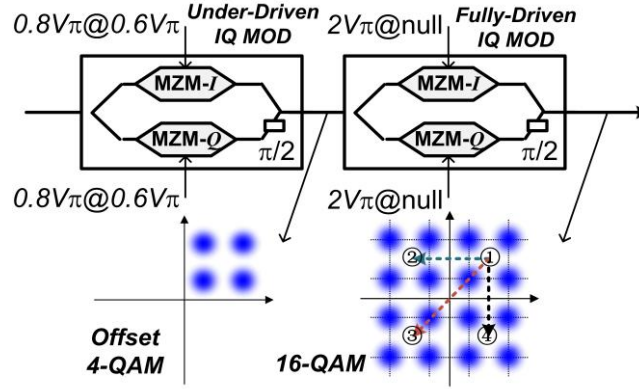
Fig. 1. Operation principle of the proposed 16-QAM transmitter using two tandem IQ modulators.

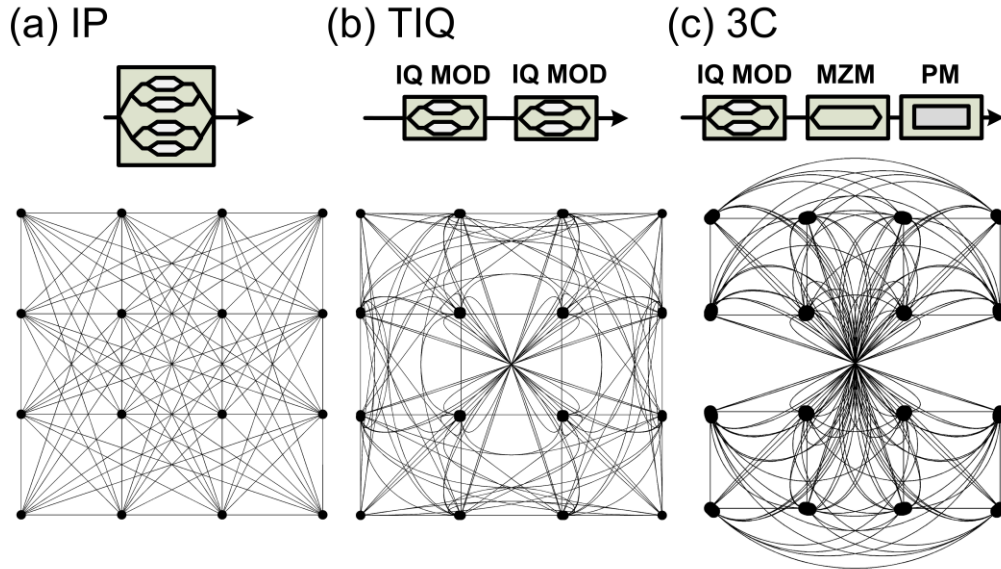## 3. Performance comparison of 16-QAM transmitters

Fig. 2. Transmitter configurations (upper) and simulated constellation diagrams (lower) of generated 16-QAM using (a) IP, (b) TIQ, and (c) 3C transmitters.

We have compared system performance of three selected 16-QAM transmitter schemes that use binary electronic signals, including: a) integrated parallel (IP) modulator [1,7,8]; b) our proposed scheme using tandem IQ (TIQ) modulators; c) three cascaded (3C) modulators, i.e. a cascade of IQ, MZM, and PM [9–11]. Figure 2 shows numerically simulated constellation diagrams of the three transmitter schemes without introducing any noise. The optical field is plotted directly after the modulator, without modeling the receiver. To see the phase transitions between the symbols, low-pass Gaussian filtering with 3-dB bandwidths of 0.65 times the symbol rate were applied at the driving electronics. Compared with the integrated IP scheme, more inter-symbol interference is observed in the TIQ and 3C transmitter schemes. It indicates that the discrete transmitter schemes, especially the 3C transmitter, are more sensitive to the bandwidth limitations of the electronics, which will be further studied below. It is seen that the transitions between the symbols are always straight lines for the IP

transmitter since all of the embedded sub-MZMs are fully-driven. However, for the cascaded schemes (TIQ and 3C), curved transitions are generated due to the deployment of an under-driven IQ modulator (TIQ and 3C) and phase modulator (3C). As will be seen later, this leads to a reduced dispersion tolerance, especially for the 3C scheme due to the deployment of a PM. We expect that by applying return-to-zero (RZ) pulse carving [12], the three constellation diagrams would be more similar.
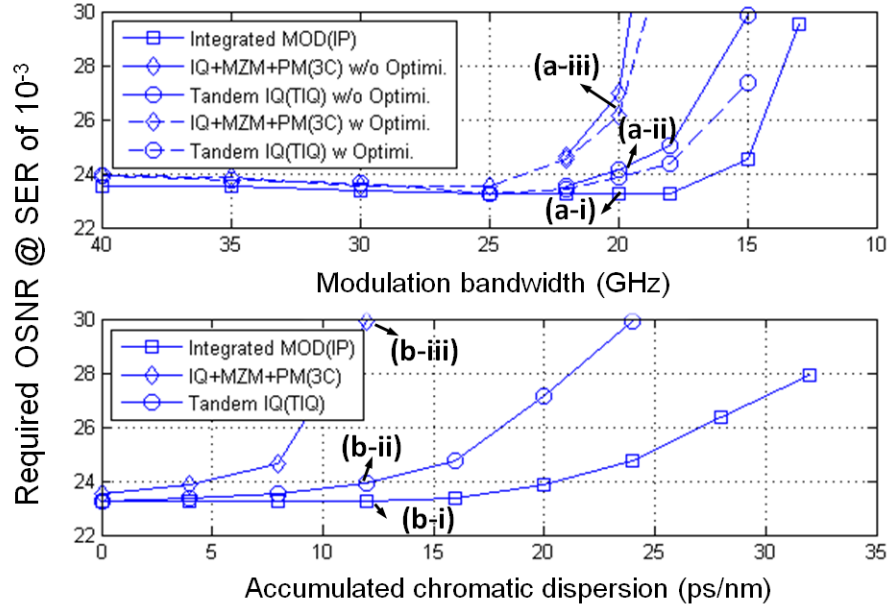

Fig. 3. Required OSNR for SER = 10^{-3} of 40-Gbaud 16-QAM as a function of (a) modulation bandwidth, and (b) accumulated chromatic dispersion. Solid lines: without optimization in the driving voltages, dashed line: with optimization in the driving voltages, square-marked: IP scheme, diamond-marked: 3C scheme, circle-marked: TIQ scheme.

A digital coherent receiver was implemented to characterize symbol-error rate (SER) in the numerical simulation at 40 Gbaud. The coherent receiver consists of optical hybrids and balanced detectors, which have 0.6-A/W responsivity, and 100-pA/√Hz thermal noise power density. The electrical filter at the receiver is 5th-order Bessel filter with 75 GHz. The response function of the driving amplifier and modulator is also 5th-order Bessel shaped. The power of the local oscillator and received signal were fixed at 10 dBm and 0 dBm, respectively. The required optical signal-to-noise ratio (OSNR) at SER of 10^{-3} is plotted as a function of the modulation bandwidth and accumulated chromatic dispersion in Figs. 3(a) and 3(b), respectively. Here, the modulation bandwidth is defined as 3-dB aggregate bandwidth of the deployed RF drivers and modulators. To investigate the impact of modulation bandwidth, no chromatic dispersion was considered. A 25-GHz modulation bandwidth was chosen for the modulators when simulating the dispersion tolerance. For the transmitter schemes 3C and TIQ, the driving voltages could be optimized to reduce the influence of the modulation bandwidth limitation. Without applying optimization in the driving voltages (shown as solid lines in Fig. 3(a)), the required modulation bandwidths at 2-dB OSNR penalty for IP, TIQ and 3C schemes are 14.6, 17.9 and 21.5 GHz, respectively. The results with the driving voltage optimization are shown as dashed lines in Fig. 3(a). Compared with the results without optimization, results were only marginally improved. The dispersion tolerance at 2-dB OSNR penalty is measured to be 25, 16.8, 8.6 ps/nm for IP, TIQ and 3C transmitter schemes, respectively. As predicted from the constellation diagrams of these schemes, the IP transmitter has the best performance, and the largest penalty was observed for the case of the 3C scheme,

in terms of tolerance against both modulation bandwidth limitation and chromatic dispersion. This is mainly because of the extra phase chirp in the TIQ and 3C transmitter schemes, especially for the 3C scheme using a cascaded PM. This is consistent with the discussion above. Figure 4(a) shows the constellations for the three transmitter schemes with 20-GHz modulation bandwidth in the absence of dispersion (points (a-i)~(a-iii) in Fig. 3), while Fig. 4(b) depicts the simulated constellations with 12-ps/nm accumulated chromatic dispersion and 25-GHz modulation bandwidth (points (b-i)~(b-iii) in Fig. 3). When introducing bandwidth limitations and chromatic dispersion, the obtained constellation using the IP scheme remains symmetric with equidistant symbols, whereas a deviation from the ideal 16-QAM grid is seen for the TIQ and 3C schemes. The constellation in the 3C scheme becomes clearly skewed.
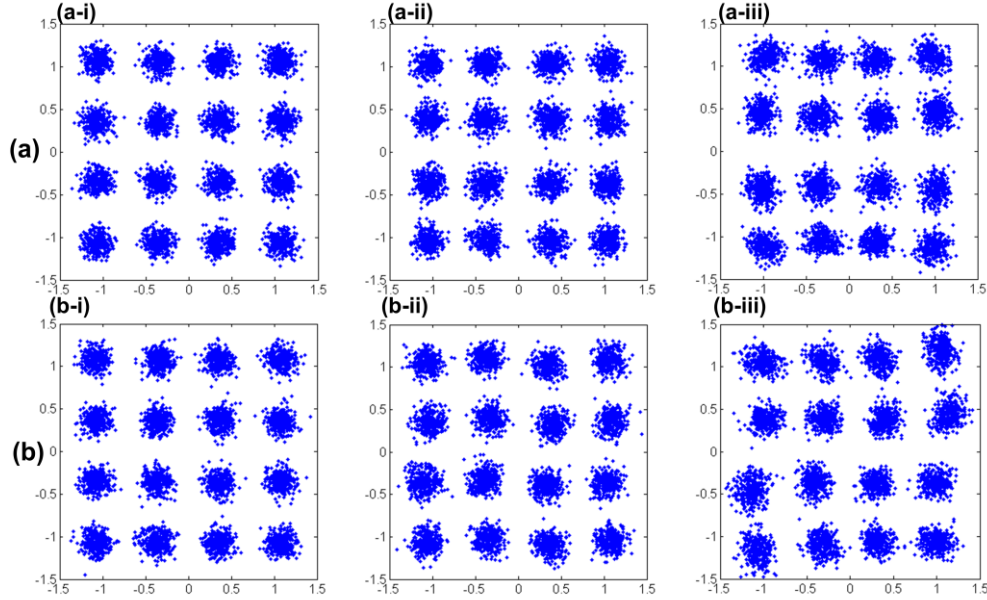

Fig. 4. Simulated constellation diagrams for three schemes with (a) 0-ps/nm accumulated chromatic dispersion and 20-GHz modulation bandwidth; (b) 12-ps/nm accumulated chromatic dispersion and 25-GHz modulation bandwidth. (a-i), (b-i): IP scheme; (a-ii), (b-ii): TIQ scheme; (a-iii), (b-iii): 3C scheme.

A theoretical study of the minimum insertion attenuation, i.e., the output-to-input power ratio, of the different transmitters has also been performed. Since all modulators are passive, the input power must be (at least) equal to the power of the symbol with the highest power. The modulation of CW light into 16-QAM therefore has a minimum attenuation of 2.6 dB, obtained by averaging over the constellation. None of the studied modulators achieve this since an IQ-modulator has 3-dB attenuation due to the fact that the electric field is split and then recombined with a $\pi/2$ phase difference. The phase modulator preserves power and an MZM will also do this when operated between maximum points, as the case is for the 3C transmitter. This leads to a total attenuation of 5.6 dB for the 3C transmitter, while the IP transmitter has attenuation of 8.1 dB. (However, if the amplitude splitting ratio is made 2:1 by design, then this number is improved to 6.0 dB.) For the TIQ transmitter the attenuation is 8.6 dB, due to the use of two cascaded IQ-modulators. When considering additional losses due to modulator non-ideality, this can impose significant OSNR degradation. One benefit of the TIQ and 3C transmitters is the possibility of inserting an amplifier in-between the two stages.
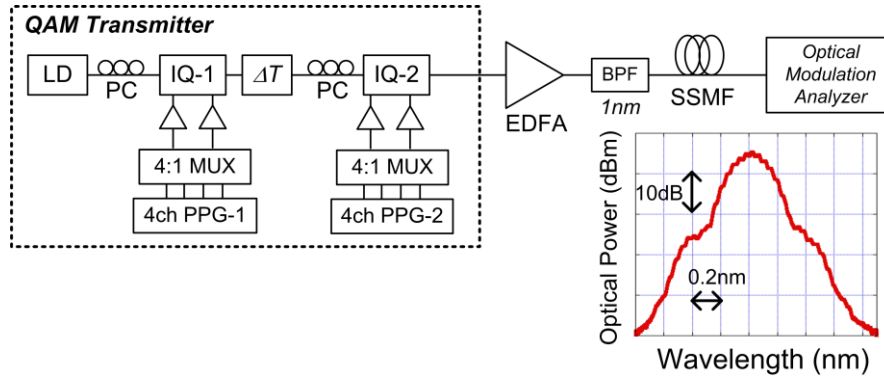
4. Experiment and results

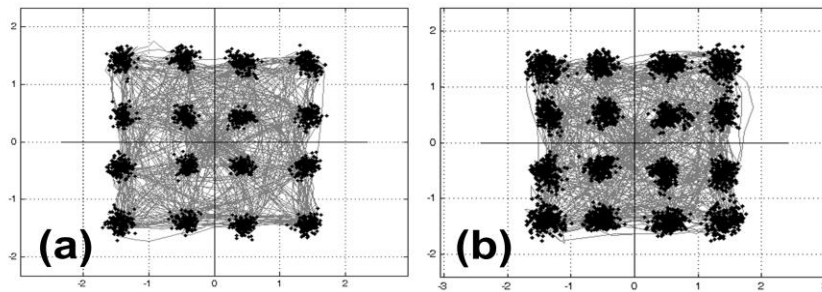Fig. 5. Experimental Setup; inset: optical spectrum of 40-Gbaud16-QAM.

Fig. 6. Measured constellations for back-to-back at (a) 28 Gbaud and (b) 40 Gbaud.

Figure 5 shows the schematic diagram of the experimental setup. A laser diode (LD) with around 100-kHz linewidth at ~1551 nm was used as signal source. 16-QAM was generated using the proposed scheme with two cascaded IQ-modulators (IQ-1 and IQ-2). The IQ modulators used in the experiment have 3-dB optical bandwidths of around 25 GHz, and half-wave voltages (V_π) of around 3.5 V. A variable optical delay (ΔT) was used to synchronize the two modulators. Electrical driving signals at 28 and 40 Gbaud were generated by applying 7-Gbit/s and 10-Gbit/s pseudorandom binary sequence (PRBS) 2^9-1 signals, respectively, to 4:1 electrical multiplexers. The pattern length was kept short to more clearly visualize the different symbol transitions in the constellation analysis. To obtain an offset 4-QAM in one quadrant, IQ-1 was under-driven using driving signals with peak-to-peak voltages of around 2.8 V. IQ-2 was fully-driven by driving signals with peak-to-peak voltages of around 7.0 V. The generated 16-QAM signal was then amplified and filtered with a bandwidth of around 1 nm before entering an equivalent-time optical modulation analyzer (EXFO PSO-200) capable of analyzing signals up to 100-Gbaud. Hence, the 40-Gbaud signal could be captured without any additional distortion. It should be pointed out that the constellations presented below represent the optical field without any ISI mitigation with DSP. Therefore, our results can be interpreted in a direct way, making e.g. comparative studies of different transmitter solutions more straightforward.

Figures 6(a) and 6(b) show the measured constellations of the 16-QAM signal at 28 Gbaud and 40 Gbaud, respectively. The symbols can be clearly distinguished from each other, which demonstrates the feasibility of the proposed 16-QAM transmitter. Due to the limited bandwidths of the employed electronics and modulators, slightly larger ISI is observed at 40 Gbaud, which is also evident in the corresponding eye diagrams of the in-phase components, shown in Fig. 7. Four levels with equal spacing are observed, as expected for an equidistant QAM constellation. The measured optical spectrum of 40-Gbaud 16-QAM is depicted in the

inset of Fig. 5. A 20-dB optical bandwidth of around 80 GHz was measured for 40-Gbaud 16-QAM. It is similar to that of binary PSK or QPSK at the same baud rate, which indicates the high spectral efficiency of 16-QAM signals.
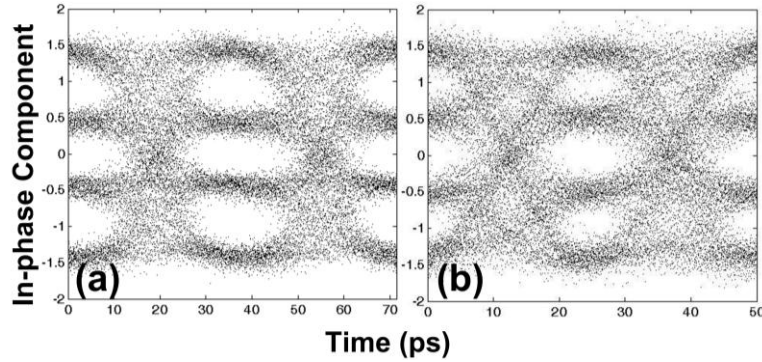

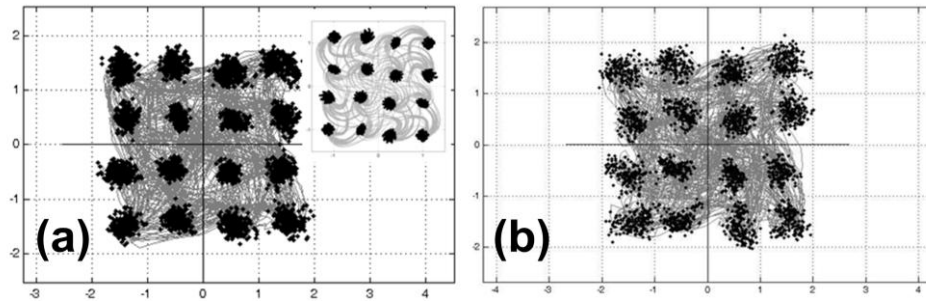Fig. 7. Measured eye diagrams of the in-phase component of (a) 28-Gbaud and (b) 40-Gbaud 16-QAM.

Fig. 8. Measured constellation of 28-Gbaud 16-QAM after transmission over (a) 1.8-km and (b) 3-km SSMF (grey line: averaged transitions, black dots: acquired symbols without averaging); inset: simulation results with fiber dispersion.

As shown in Fig. 8, after passing through the SSMF the measured symbols of 28-Gbaud 16-QAM were scattered due to the introduced dispersion. As seen from the averaged transitions shown by grey lines in the figure, "s"-shape phase spirals are observed at the symbol transitions in the constellation. This is expected from the numerical simulations with same amount of dispersion, see the inset of Fig. 8(a).

5. Conclusion

We have proposed and experimentally demonstrated a novel 16-QAM transmitter based on two cascaded IQ modulators driven by four separate binary electrical signals. For the first time, 16-QAM signals at 40 Gbaud were successfully generated and analyzed with a high speed constellation analyzer. Compared with the integrated IP, the proposed scheme shows slightly worse performance in simulations, but on the other hand, it outperforms the cascaded 3C scheme, regarding tolerance to modulation bandwidth limitations and chromatic dispersion. The scheme features scalable configuration and stable performance with simple bias-control.